

151 XOMO  
1 copy

# THE ARMORING PROCESS ON THE FALL RIVER



WRD REPORT NO. 86-4



WATER RESOURCES DIVISION  
NATIONAL PARK SERVICE  
COLORADO STATE UNIVERSITY  
FORT COLLINS, COLORADO 80523

This report presents the results of a study conducted by the National Park Service Water Resources Division. It is intended primarily for use by the particular Park Service area or areas that are addressed in the report but may be of interest to other persons working in water resources management. Requests for copies of this report should be addressed to:

Chief  
Water Resources Division  
National Park Service  
301 South Howes Street  
Fort Collins, Colorado 80521

Note: Use of trade names does not imply U.S. Government endorsement of commercial products.

THE ARMORING PROCESS ON THE FALL RIVER

WRD Report No. 86-4

Submitted

As Fulfillment of the Requirements

for CE695B

Independent Study - Hydraulics

by


Kenton J. Bruxvoort  
Department of Civil Engineering  
Colorado State University

and

Colin R. Thorne  
Department of Geography and Earth Science  
Queen Mary College, University of London

January 1986

National Park Service  
Water Resources Division  
Colorado State University  
Fort Collins, Colorado 80523



Digitized by the Internet Archive  
in 2012 with funding from  
LYRASIS Members and Sloan Foundation

<http://archive.org/details/armoringprocesso00brux>

## ACKNOWLEDGMENTS

The author would like to thank Tom Ochwat and John Charette for their assistance in data collection. The guidance given me by Jeff Bradley was essential in allowing me to complete this paper. Moreover, the information, help and equipment given to me by John Pitlick were all gratefully received. Special thanks is given to Dr. Steven Abt, my major advisor, for the advice given at different phases of this study; to Drs. Johannes Gessler and Mike Harvey for their aiding in my understanding; and to Dr. Colin Thorne for his patience with me, for his counsel, and for his humor.



# TABLE OF CONTENTS

	<u>Page</u>
Acknowledgment . . . . .	ii
List of Tables . . . . .	iv
List of Figures . . . . .	v
1.0 Introduction . . . . .	1
1.1 Scope of This Paper . . . . .	1
1.2 Project Background and Description . . . . .	1
1.3 Description of the Study Reach . . . . .	4
2.0 The Armoring Process . . . . .	6
2.1 Discussion of Armoring and Paving . . . . .	6
2.2 Presentation of the Models . . . . .	8
3.0 Data Collection . . . . .	10
3.1 Description of the Data Collection Technique . . . . .	10
3.2 Presentation and Discussion of the Data . . . . .	11
4.0 Application of the Models . . . . .	23
4.1 Results of the Application . . . . .	23
4.2 Discussion of Results . . . . .	26
5.0 Summary . . . . .	28
Bibliography . . . . .	30
Appendix A . . . . .	31
Appendix B . . . . .	38





# LIST OF TABLES

<u>Table</u>		<u>Page</u>
1	Field Results, Bed Material Grain Size Distribution . .	12
2	Field Results, $d_{50}$ For Each Cross Section . . . . .	13
3	Initial Grain Size Distribution . . . . .	24
4	Comparison of Observed and Predicted $d_{50}$ . . . . .	26
5	Hydraulic Radii and Mean Bed Shear Stresses for the Five Cross Sections . . . . .	33
6	Armor Layer Computations, $P_a$ , Cross Section 7 (Gessler) . . . . .	34
7	Armor Layer Computations, $P_a$ , Cross Section 5 (Shen) . .	35



# LIST OF FIGURES

<u>Figure</u>		<u>Page</u>
1	Map Sketch of the Roaring River Area . . . . .	2
2	Map Sketch of the Study Reach . . . . .	5
3	Grain Size Distributions, Cross Section 3 . . . . .	14
4	Grain Size Distributions, Cross Section 5 . . . . .	15
5	Grain Size Distributions, Cross Section 7 . . . . .	16
6	Grain Size Distributions, Cross Section 9 . . . . .	17
7	Grain Size Distributions, Cross Section 11 . . . . .	18
8	Fall River Runoff Hydrograph for 1983, 1984 and 20-year Average . . . . .	21
9	Initial Grain Size Distributions . . . . .	25
10	Prediction of Armor Layer (Gessler) . . . . .	36
11	Prediction of Armor Layer (Shen) . . . . .	37
12	Size Distribution Curve, Cross Section 2, 1983 . . . . .	39
13	Size Distribution Curve, Cross Section 4, 1983 . . . . .	40
14	Size Distribution Curve, Cross Section 6, 1983 . . . . .	41
15	Size Distribution Curve, Cross Section 9, 1983 . . . . .	42
16	Size Distribution Curve, Cross Section 11, 1983 . . . . .	43
17	Variation in $d_{50}$ , 1983 . . . . .	44



## 1.0 INTRODUCTION

### 1.1 Scope of This Paper

By studying the extent of the armoring process in a gravel-bed river, an engineer or a geomorphologist can predict the stability of the bed. It is desirable to know the stability of a gravel bed to gain an understanding of the degree of degradation which can be expected.

This paper describes the degree of armoring on a particularly dynamic stretch of the Fall River in Rocky Mountain National Park. It also compares models presented by Gessler (1970) and Shen (1983) to predict the extent to which a gravel bed will armor. The two models are then applied to this stretch of the Fall River and compared to data collected at the same site during the summer of 1984.

### 1.2 Project Background and Description

On July 15, 1982, an earth-fill dam impounding Lawn Lake in Rocky Mountain National Park burst, releasing nearly 700 acre-feet of water into the Roaring River. This event, much larger than any runoff event since the melting of the glaciers several thousand years ago, gouged the Roaring River valley to bedrock, removing as much as 80 feet of glacial moraine. The Roaring River, a small, steep river with a bed of gravel, cobbles and boulders, joins the Fall River approximately five miles below Lawn Lake. Just upstream of the confluence, a major canyon was cut and the material eroded was deposited in a large alluvial fan containing boulders as large as 20 feet in diameter, but grading to sand and silt within about 1000 feet. This fan ponded behind it a portion of the Fall River, forming Flood Lake. The Roaring River becomes braided as it crosses the fan and joins the Fall River at the toe of the fan (Fig. 1).



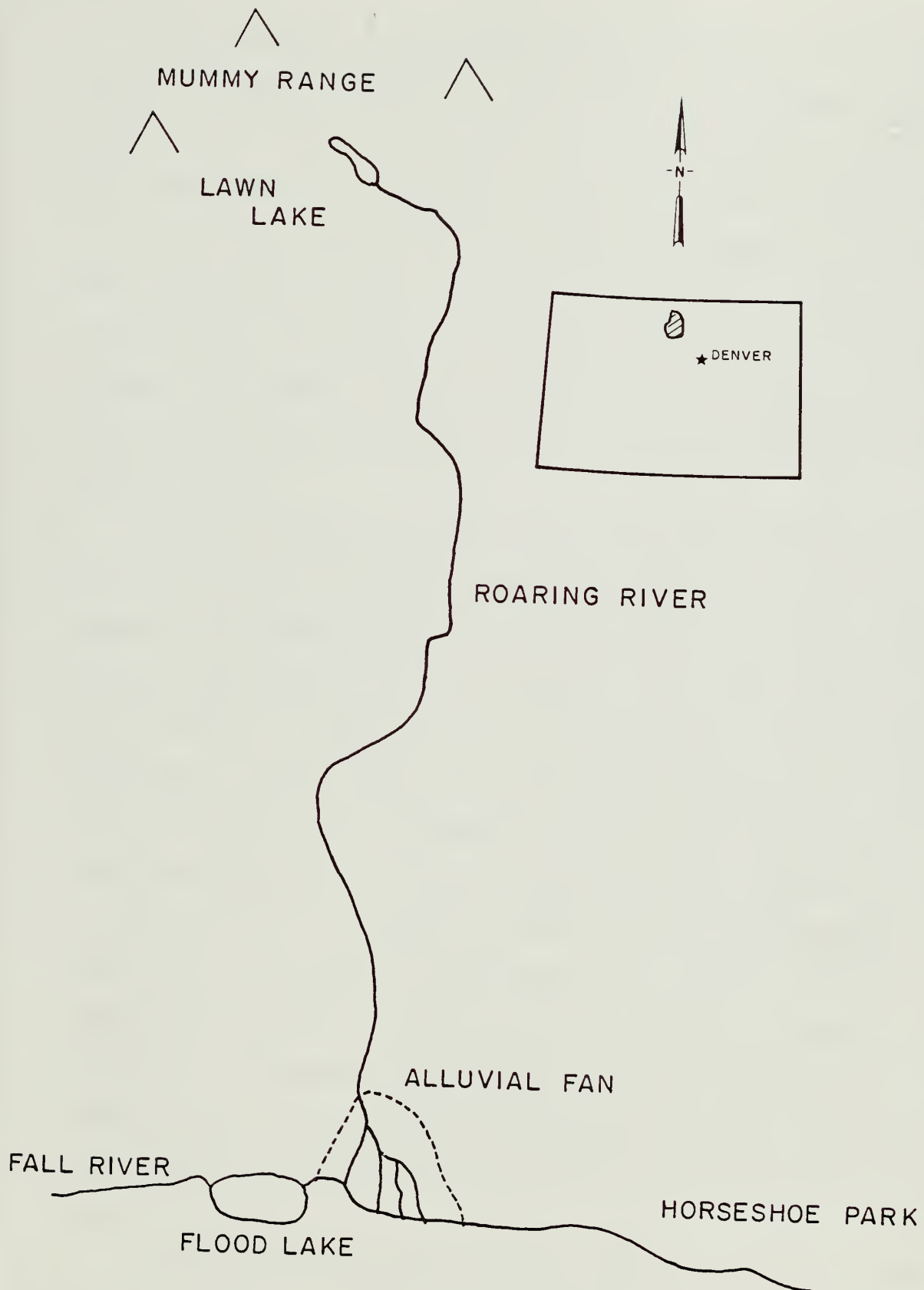


Figure 1. Map Sketch of the Roaring River Area





The confluence of the Roaring and Fall Rivers is in a wide, glaciated valley called Horseshoe Park. This name is derived from the highly sinuous nature of the river as it eases through the relatively flat valley floor. The Lawn Lake floodwaters roared into Horseshoe Park but ponded there because of the low gradient and backwater from Cascade Dam at the end of the park. After Cascade Dam failed the waters rushed on downstream to Estes Park, finally being captured in Lake Estes behind Olympus Dam. Because of the low velocities in the ponded flow, the floodwaters had little impact on the Fall River downstream of the fan in Horseshoe Park.

During the summers of 1983 and 1984 faculty and graduate students of Colorado State University conducted geomorphic and sedimentation studies of the Roaring River valley, the alluvial fan area, Horseshoe Park and further down the Fall River valley to Lake Estes. In addition, the Institute of Hydrology in the United Kingdom sent a team of scientists to jointly study, with the Colorado State University contingent, the behavior of the sedimentation occurring in the Roaring River. The unique responses to sediments of gravel-bed rivers, and particularly of this one, were of interest to these scientists who were funded in part by the North Atlantic Treaty Organization. The Fall River Project studies have included an examination of the geomorphic responses of the Fall River in Horseshoe Park following the flood, determination of sediment motion in Horseshoe Park and downstream of there to Lake Estes, and a study of the stability of the high, steep banks of the Roaring River.

In addition, the armor layer was studied in the reach which extends from just below the outlet of Flood Lake approximately 650 feet downstream. A report was published detailing the results of the 1983 study



on the armoring of the bed in this reach (Biedenharn, 1983). The fieldwork performed in 1984 and this report are a part of this on-going research effort.

### 1.3 Description of the Study Reach

The study reach, shown in Figure 2, is located in the Fall River at the very toe of the alluvial fan. This 650 foot-long reach was divided into 11 cross sections for research purposes. For this study, five of these cross sections were chosen: cross section numbers three, five, seven, nine and eleven (Fig. 2).

This reach has a highly mobile bed material for two reasons. First, there is a plentiful, but unsteady supply of sediment from upstream. Sediment load is carried into the reach due to the erosion caused by high flows during the early summer snowmelt and high flows during thunderstorms. In addition, the thunderstorm runoff causes sheet and rill erosion on the unstable canyon walls and across the alluvial fan. Sediment loads are quite small in August, for example, after the snowmelt has receded, but may increase rapidly due to the occurrence of a flash flood caused by a thunderstorm. Second, the locations and flow distributions of the Roaring River inflows to the Fall River are quite variable. For example, whereas almost all of the Roaring River flow entered the study reach between cross sections three and seven before a July 24, 1984 thunderstorm, afterward most of it entered above cross section three. Thus, for both these reasons, the amount of sand and fine gravel making up the bed and bedload at the different cross sections varies widely.



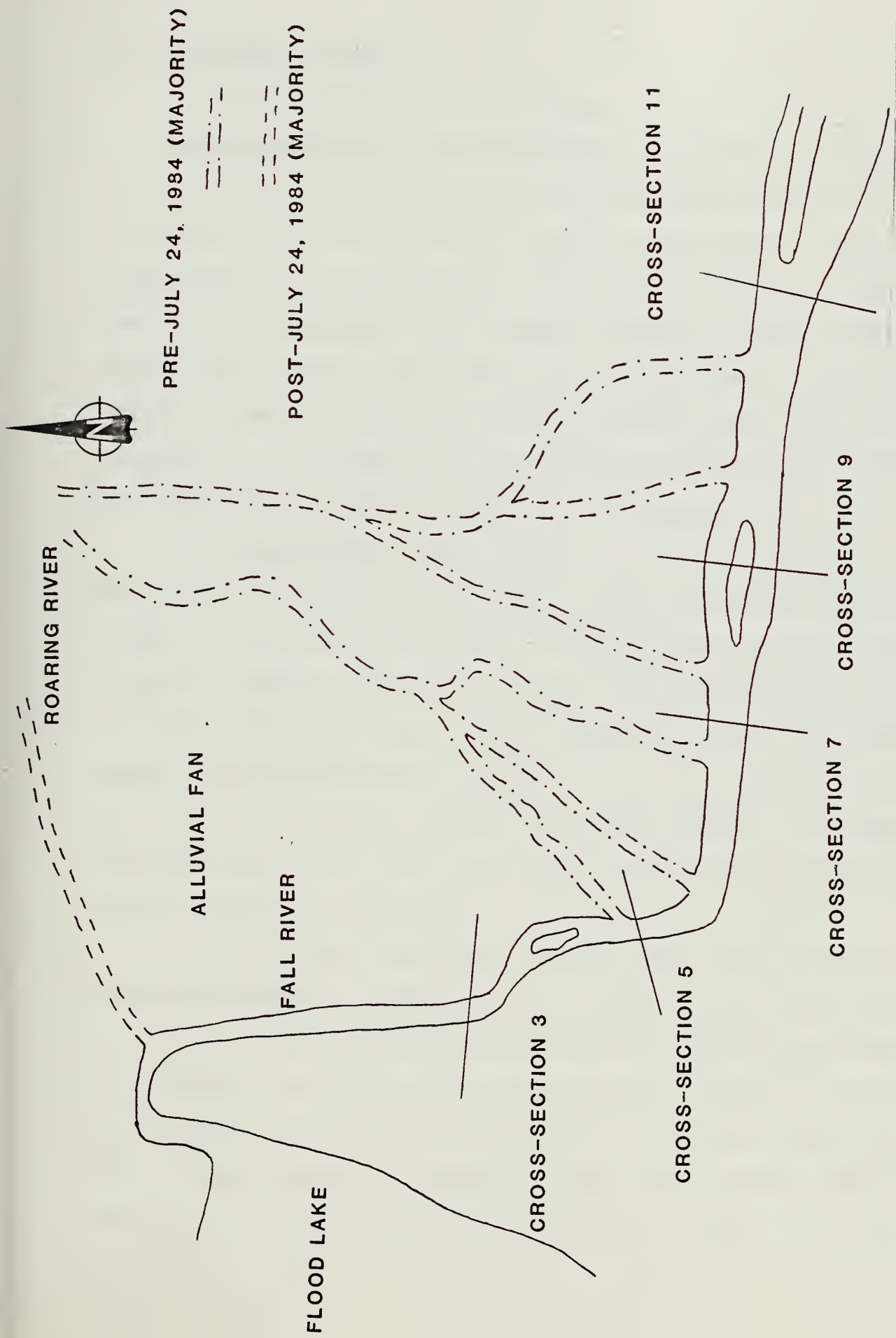


Figure 2. Map Sketch of the Study Reach



## 2.0 THE ARMORING PROCESS

### 2.1 Discussion of Armoring and Paving

Incipient motion of a particle situated on a stream bed occurs when the shear stress exerted on the particle by the flow of water over it is just equal to the critical shear stress for that particle. Critical shear stress is a function of the weight and diameter of the particle and the size distribution of the sediment mixture. It can be approximated using a graph of the dimensionless critical shear stress, or Shields parameter, versus the particle Reynolds number (ASCE Task Committee for the Preparation of the Manual on Sedimentation, 1975). This dimensionless graph is called the Shields diagram.

In a coarse-bedded stream, motion of the finer grains of the material is more likely to occur before motion of the coarser grains because of their lower critical shear stress and greater mobility. This process of winnowing the smaller particles from the mixture is called armoring. After some time, selective removal of the finer grains results in the generation of a relatively stable coarse surface layer protecting the underlying sediment from further erosion. No further degradation will occur until the arrival of an event sufficiently extreme to break the armor layer.

In analyzing this coarse layer, Bray and Church (1980) proposed a delineation between an armor layer and a pavement. They defined the armor layer to exist if the subsurface material, with the grain size distribution truncated below 8 mm, had essentially the same distribution as the surface material. The surface layer is a pavement, however, if the subsurface material, excluding the grain size distribution below 8 mm, is noticeably finer than the surface material. By these





definitions, an armored bed is mobile at high flows, while a paved bed is essentially immobile.

The state of mobility of the bed controls the number of degrees of freedom of a stream. An armor layer is, by the above definition, still undergoing a certain amount of bed material movement, so that a particular stretch of river may be able to move not only laterally, but vertically as well. A pavement, on the other hand, limits the stretch of river to one degree of freedom, that of lateral movement only. The pavement allows for no further degradation, even under flows of extremely large magnitude. Breakup of a pavement may occur over a period of time encompassing thousands of years whereas breakup of an armor may occur during a storm event.

This definition of terms is, however, not universally accepted. Early researchers made no reference to the difference between armored and paved gravel beds. Most researchers simply refer to the coarse surface layer in a stream as armored. Parker (1981) makes note of this, paying tribute to the "time-honored usage" of the term "armored" in describing the coarse surface material developed downstream of dams. But, he also believes it wise to note the difference between the two terms. However, he reverses the definitions from those above. In his publications, he uses the word "armored" to describe a relatively permanent bed cover and the word "paved" to describe a more mobile stream bed. This can be the source of much confusion. Consequently, it is wise to clarify the terminology used in any particular report.

In describing the bed material on the test reach of the Fall River the terms as defined by Parker (1981) and previous writers are used because the author believes that that usage has taken root in the literature and will remain there.



## 2.2 Presentation of the Models

Often, mathematical models are used to predict the behavior of physical processes. The parameters which affect the process are grouped together in a mathematical expression, which is then tested experimentally. By then measuring the parameters, whether they be discharge, depth of water or size of an object, and applying them to the model, scientists can gauge how the process will respond.

Gessler (1970) proposed a statistical model for analyzing the armoring of bed material by defining the probability that a particular grain will remain a part of the bed. Movement of a bed particle is a function of the probability that the local shear stress is less than the critical shear stress for incipient motion of that particular grain. If the critical shear stress exceeds the local shear stress exerted by the water on the grain, it will remain in the bed. Particle movement is also a function of the initial grain size distribution of the bed material. The size distribution of the armor layer is then described by:

$$p_a(k) = \frac{\int_{k_{\min}}^k q p_o dk}{\int_{k_{\min}}^{k_{\max}} q p_o dk}, \quad (1)$$

where  $p_o$  is the initial grain size distribution,  $k$  is the grain diameter,  $k_{\min}$  and  $k_{\max}$  are the lower and upper bounds of the integration of the grain size distribution, and  $q$  is the probability of movement of a bed particle. In this relationship  $q$  is given by:

$$q(\tau < \tau_c) = \frac{1}{\sigma\sqrt{2\pi}} \int_{-\infty}^{(\tau_c/\bar{\tau})-1} \exp\left(-\frac{x^2}{2\sigma^2}\right) dx, \quad (2)$$



where  $\tau$  is the local shear stress,  $\tau_c$  is the critical shear stress of the grain,  $\bar{\tau}$  is the mean bed shear stress,  $\sigma$  is the standard deviation of the shear stress fluctuation, and  $x$  is a dummy variable. The critical shear stress is found, as mentioned earlier, from the Shields diagram. The grain Reynolds number in the Shields diagram is given by:

$$R_{e_*} = \frac{U_* d_s}{\nu}, \quad (3)$$

where  $U_*$  is the shear velocity,  $d_s$  is the representative particle diameter, and  $\nu$  is the kinematic viscosity of the water. Experimentally, Gessler (1970) found the standard deviation of the shear stress fluctuations to be  $\sigma = 0.57 \bar{\tau}$ .

This probability of movement of a bed particle,  $q$ , was assumed to be normally distributed. The value of  $q$  for a particular grain could therefore be found by normalizing the upper bound of the integral and then using normal probability distribution tables. Movement of a particle would just occur when the value of  $q(k) = 0.50$ .

Shen (1983) proposed three modifications to Gessler's model. First, he modified the Shields diagram, which is based on uniform material, to account for nonuniform material. Second, he introduced Einstein's hiding factor into the procedure. The hiding factor accounts for the tendency of smaller particles to be shielded from some of the shearing action of the flow by "hiding" behind larger particles. Third, he considered that different initial grain size distributions are affected by shear stress fluctuations differently. Therefore, the standard deviation of the shear stress fluctuations should not be only a function of the shear stress mean. The probability that the local shear stress on a particle is less than the critical shear stress is then given by:



$$q(\tau < \tau_c) = \frac{1}{\sqrt{2\pi}} \int_{-\infty}^{X_u} \exp(-\frac{x^2}{2}) dx , \quad (4)$$

in which,

$$X_u = \frac{\xi(\tau_c/\bar{\tau} - 1)}{(CV)_\tau} . \quad (5)$$

It should be noted that  $\tau_c$  is to be found from Shen's modified Shields diagram;  $\xi$  is Einstein's hiding factor and is found using part of Einstein's procedure for predicting sediment bedload (ASCE Task Committee, 1975); and the coefficient of variation,  $(CV)_\tau$ , is a function of the standard deviation of the initial grain size distribution (Shen, 1983).

The two models were applied to the armoring observed on the Fall River, to test their effectiveness. Before applying the methods though, it is necessary to describe how the field data were collected, and to present the data.

### 3.0 DATA COLLECTION

#### 3.1 Description of the Data Collection Technique

The grid-by-number method devised by Wolman (Kellerhals and Bray, 1971) was used to determine the grain size distribution of the surface bed material. Kellerhals and Bray recommended this procedure primarily because of its equivalence to bulk sieve analysis. Using this technique, results obtained in the field can be readily compared with a laboratory sieve analysis.

In the grid-by-number technique the person doing the sampling selects a representative, random sample of the bed material. The grid is established by pacing, and covers the whole sampling area evenly.





The sampler paces from bank to bank and back, working his way downstream. Each pebble is selected by removing the particle located just in front of the toe of the boot, with the sampler's eyes averted. The stone is passed through a gravelometer developed by Hey and Thorne (1983) and returned to the bed. One hundred stones are selected at each cross section. Using this technique no stone is sampled twice.

The gravelometer allows measurement of the intermediate axis of the stone, by noting the size of the smallest aperture through which the stone will pass. The use of the gravelometer precludes sampler errors involved in selecting and measuring intermediate axes with a ruler or calipers, and is a much faster method as well. However, it does produce systematically smaller results than would be obtained with ruler or calipers since the stone can pass diagonally through the square hole.

### 3.2 Presentation and Discussion of the Data

Bed material size distributions were collected on three separate occasions: June 16, July 19, and August 21, 1984. On June 16, samples were collected at cross sections five, nine, and eleven; on July 19, cross sections three, five, seven, and nine were sampled; and on August 21, all five cross sections were sampled. The distributions of the bed material grain sizes are shown in Table 1. Table 2 displays the median diameter size,  $d_{50}$ , for each distribution, based on the field data. In addition, Figs. 3-7 display the plots of the grain size distribution for each cross section, showing how the distributions changed from month to month.

In Figs. 3-7, the distributions are truncated below 8 mm. This is done for three reasons. First, the exact distribution of the bed material below this cutoff point is not crucial to know when one is



Table 1. Field Results, Bed Material Grain Size Distribution

July 16, 1984					
Cross Section 5		Cross Section 9		Cross Section 11	
D, mm	% Finer	D, mm	% Finer	D, mm	% Finer
256	100	256	100	256	100
180	98	180	100	180	99
128	90	128	94	128	97
90	69	90	85	90	77
64	48	64	67	64	56
45	28	45	49	45	33
32	14	32	30	32	24
22.5	3	22.5	16	22.5	12
16	1	16	3	16	8
11.2	0	11.2	2	11.2	5
		8	1	8	2
				5.6	1
				4	0
		2	0		

July 19, 1984							
Cross Section 3		Cross Section 5		Cross Section 7		Cross Section 9	
D, mm	% Finer	D, mm	% Finer	D, mm	% Finer	D, mm	% Finer
256	100	256	100	256	100	256	100
180	95	180	98	180	99	180	100
128	85	128	94	128	94	128	98
90	70	90	86	90	91	90	89
64	58	64	71	64	76	64	76
45	45	45	58	45	63	45	62
32	35	32	33	32	53	32	49
22.5	24	22.5	16	22.5	36	22.5	40
16	17	16	8	16	24	16	25
11.2	11	11.2	3	11.2	17	11.2	19
8	9	8	2	8	10	8	13
5.6	7	5.6	1	5.6	5	5.6	10
4	3			4	3	4	7
				2.8	2	2.8	5
2	0	2	0	2	0	2	0



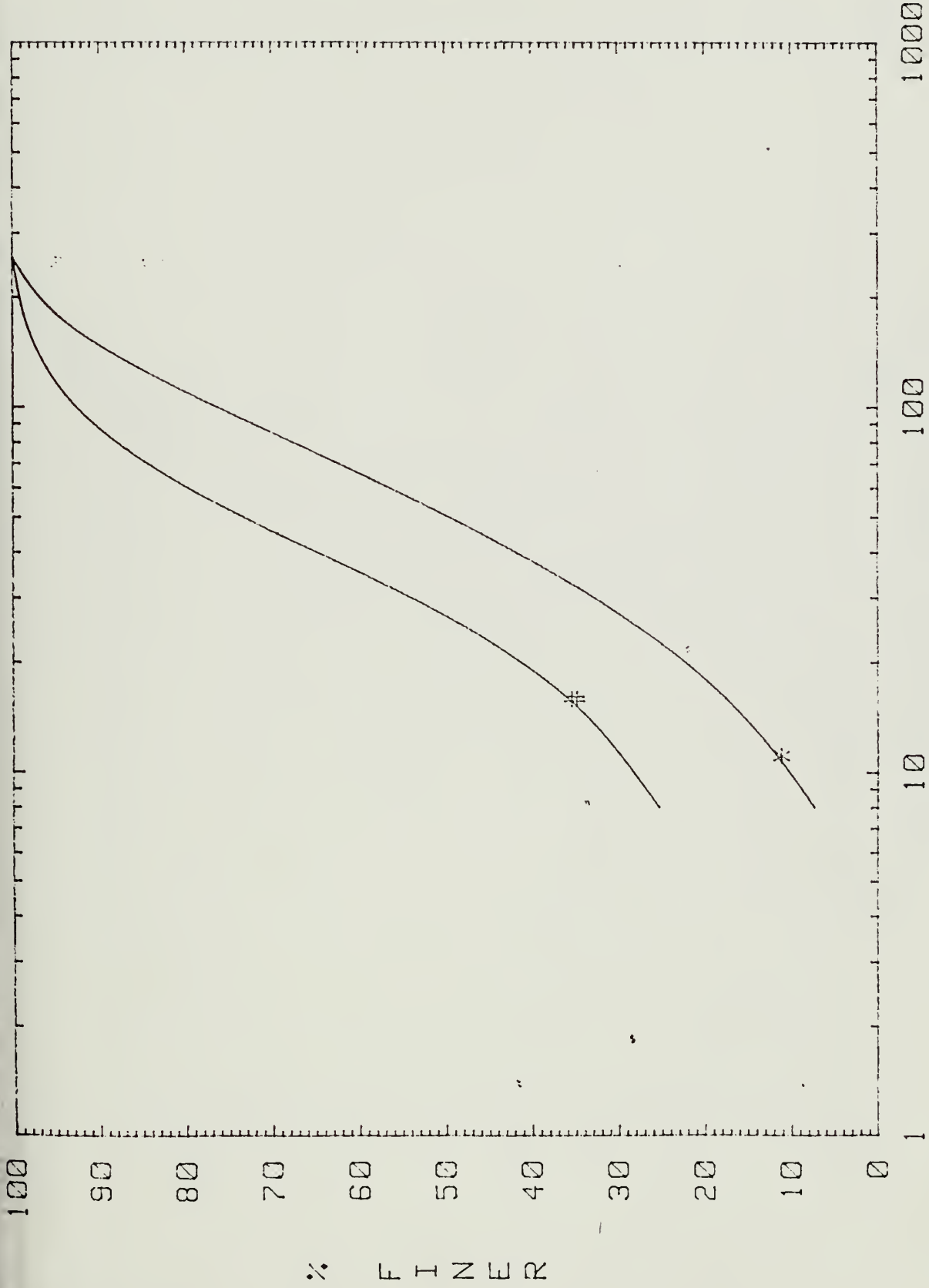
Table 1. Continued

August 21, 1984									
Cross Section 3		Cross Section 5		Cross Section 7		Cross Section 9		Cross Section 11	
D, mm	% Finer	D, mm	% Finer	D, mm	% Finer	D, mm	% Finer	D, mm	% Finer
256	99	256	100	256	100	256	100	256	100
180	--	180	100	180	100	180	100	180	100
128	96	128	94	128	99	128	99	128	99
90	92	90	87	90	85	90	93	90	97
64	82	64	81	64	75	64	74	64	95
45	71	45	65	45	50	45	62	45	78
32	54	32	53	32	38	32	51	32	64
22.5	44	22.5	43	22.5	22	22.5	40	22.5	44
16	35	16	32	16	8	16	32	16	27
11.2	30	11.2	27	11.2	7	11.2	24	11.2	19
8	26	8	23	8	5	8	17	8	15
5.6	21	5.6	18	5.6	3	5.6	13	5.6	12
4	15	4	11			4	12	4	10
2.8	13	2.8	8			2.8	10	2.8	6
2	0	2	0	2	0	2	0	2	0

Table 2. Field Results,  $d_{50}$  for Each Cross Section

Date	X-Sect. 3 $d_{50}$ , mm	X-Sect. 5 $d_{50}$ , mm	X-Sect. 7 $d_{50}$ , mm	X-Sect. 9 $d_{50}$ , mm	X-Sect. 11 $d_{50}$ , mm
6/16/84		66		46	59
7/19/84	47	40	31	32	
8/21/84	27	28	42	31	25



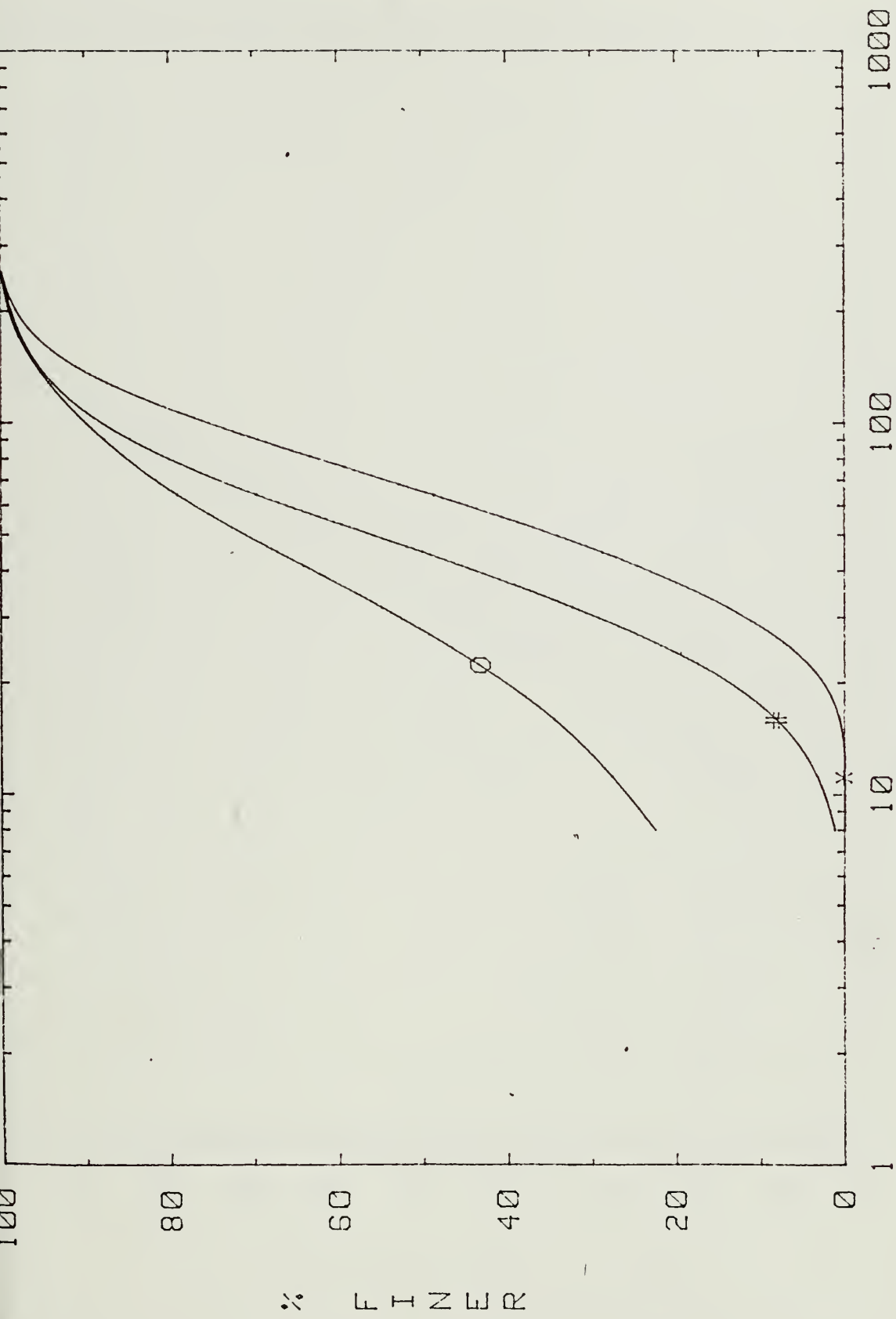


\* DATE: 7/19/84  
BED MATERIAL DIAMETER, mm  
# DATE: 8/21/84

Figure 3. Grain Size Distributions, Cross Section 3



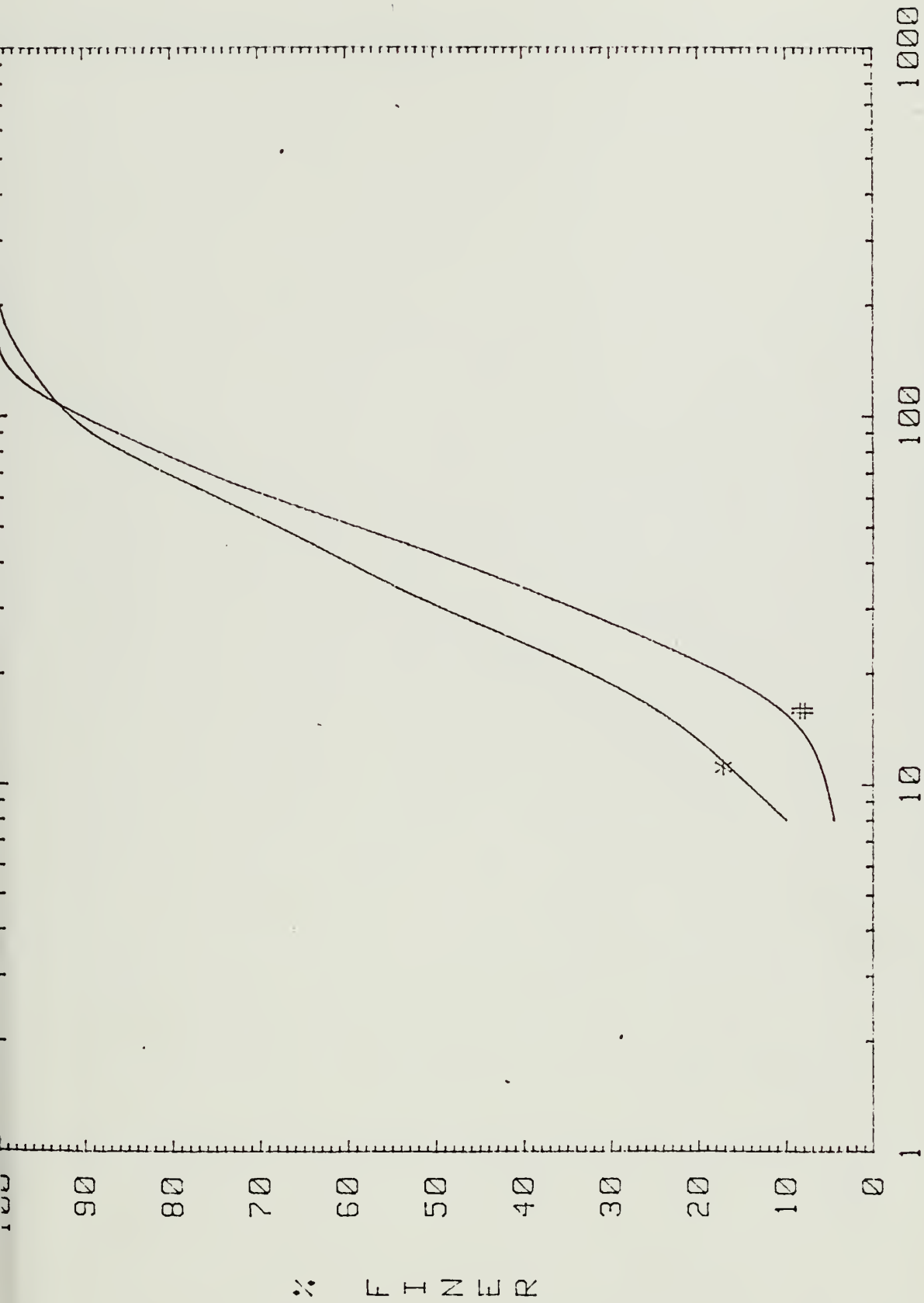




\* DATE: 6/16/84  
 BED MATERIAL DIAMETER, mm  
 # DATE: 7/19/84  
 O DATE: 8/21/84

Figure 4. Grain Size Distributions, Cross Section 5

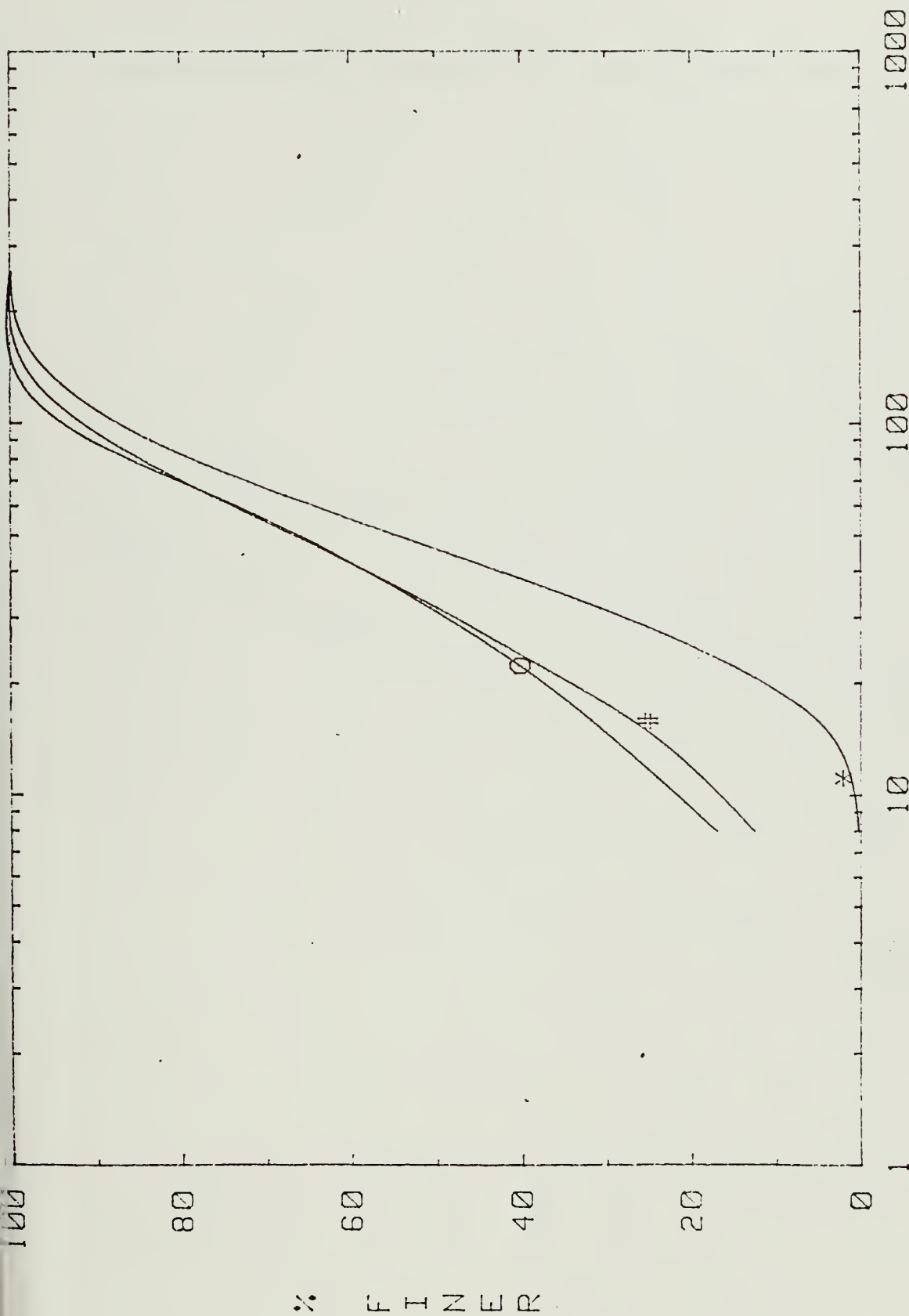




\* DATE: 7/19/84  
 BED MATERIAL DIAMETER, mm  
 # DATE: 8/21/84

Figure 5. Grain Size Distributions, Cross Section 7

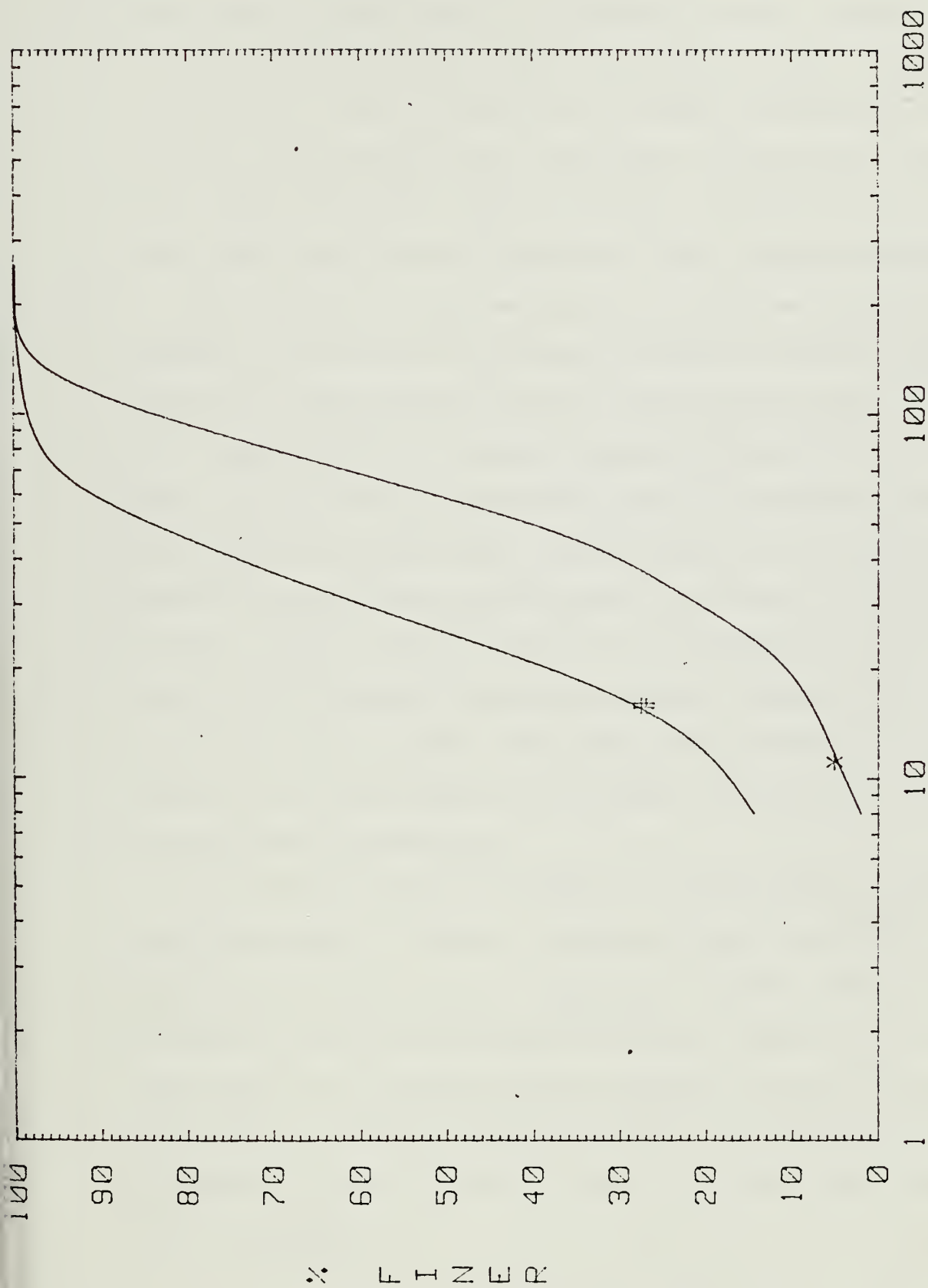




\* DATE: 6/16/84  
 BED MATERIAL DIAMETER, mm  
 # DATE: 7/19/84  
 O DATE: 8/21/84

Figure 6. Grain Size Distributions, Cross Section 9





\* DATE: 6/16/84  
BED MATERIAL DIAMETER, mm  
# DATE: 8/21/84

Figure 7. Grain Size Distributions, Cross Section 11





describing an armor layer in a gravel-bed stream. Second, it is difficult to get an accurate count of material less than 8 mm diameter in the field. This is because of difficulty in picking the finest particles out of the bed due to their small size and due to the cold water temperature which numbs the fingers. Third, Bray and Church (1980) make note of the 8 mm truncation in their article cited earlier.

The composition of the bed material in the test reach is highly dependent on the amount of sediment load which is delivered from the alluvial fan. The sediment transport capability of the reach is, therefore, supply-limited, as opposed to transport-limited (Pitlick, 1985). When a portion of the flow changes its path, it erodes material which it then carries to the Fall River. This rebraiding of the Roaring River initially decreases the size distribution of the surface bed material in the fan. As time goes by, however, the newly-formed bed develops a paving as the fines are transported downstream. Sediment load to the test reach is then lessened. The water flowing through the reach is very nearly like the sediment-free discharge just downstream of a dam. An armored bed can then develop.

As reported by Biedenharn (1983), on the Fall River bed material, during the summer of 1983 the locations of the Roaring River flows across the fan varied greatly. Consequently, the mean diameter of the bed material also varied throughout the summer. The bed did not become always coarser but alternated between becoming finer and then becoming coarser again. There was, however, an overall coarsening trend in these fluctuations. This is shown in Figs. 12-17, taken from Biedenharn (1983), in Appendix B.



During the summer of 1984, however, the Roaring River did not change its course across the fan in the same way as it did in 1983. This is tied to, although probably not wholly, to the fact that 1983 experienced much more runoff, with higher peaks, than did 1984 (Pitlick, 1985). This is depicted in Fig. 8. Only once in 1984 did the Roaring River appreciably change the location of its braids. This happened during a thunderstorm that occurred on July 24, 1984. Before this thunderstorm, most of the Roaring River flow joined the Fall River between cross-sections three and seven. After it, most of the Roaring River flow entered above cross section three, just downstream of Flood Lake.

Consequently, most of the sediment coming from the alluvial fan in 1984 came from sheet and rill erosion on the fan, with an appreciably lesser amount coming from the beds of the Roaring River braids. The amount of sediment input to the test reach was still quite variable, but the process by which it was being derived changed. Whereas in the summer of 1983 erosion of material on the fan was caused by both sheet erosion and river bed erosion, in the summer of 1984 erosion occurred mainly by sheet erosion alone. The erosion caused by the July 24, 1984 event was the primary exception to this general rule. Table 2, given previously, displays the variation in  $d_{50}$  throughout the summer for the five cross sections.

At cross section three, the bed material size distribution was coarser on July 19, 1984 than on August 21, 1984. On July 19, most of the Roaring River flow, with its sediment load from the fan and from the valley upstream, entered below this cross section. Therefore, the Fall River water at this cross section resembled the clear water discharge downstream of a dam because little sediment is brought by the Fall River



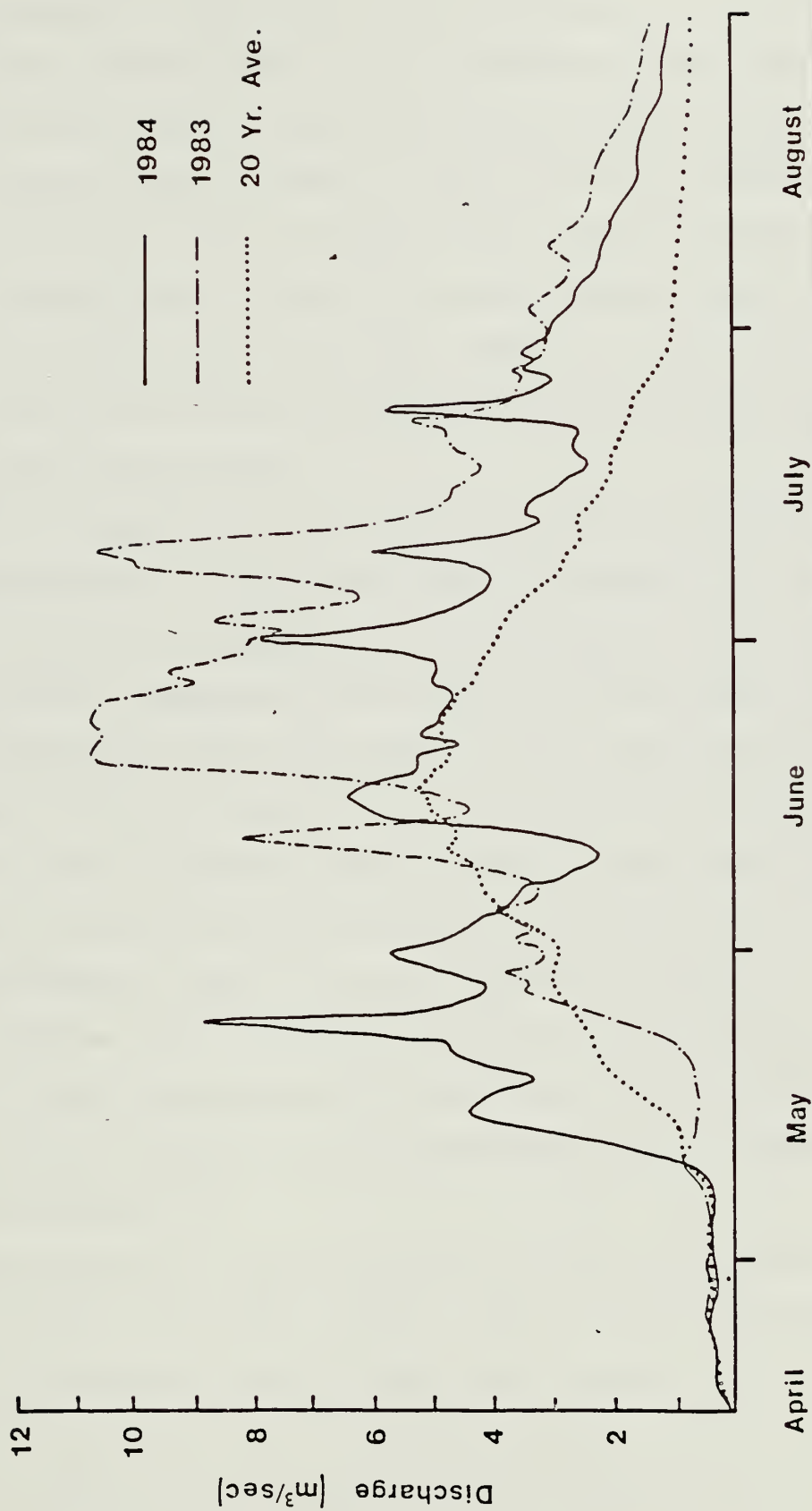


Figure 8. Fall River Runoff Hydrograph for 1983, 1984 and 20-year Average (From Pitlick, 1985)



from upstream to Flood Lake and the discharge at the outlet is essentially sediment-free. This was evidenced by some algal growth along the bed, which is characteristic of an armored gravel bed with little sediment input or removal. After July 24, 1984, with the transposition of much of the Roaring River flows to upstream of cross section three, sediment load to this cross section increased greatly. Consequently, the bed became much finer. The armor layer still existed intact, but it was partially overlain by some finer material which was input from erosion upstream.

The bed material in cross section five also became finer as the summer progressed. It can be noted that its bed material size distributions for July 19 and August 21, 1984 are similar to those for cross section three. (Comparison of June, 1984 data cannot be made as no data were collected for cross section three in June.) This similarity exists because both cross sections were affected in the same way by the dynamics of the alluvial fan. Based on this, it might be predicted that the  $d_{50}$  of the bed material for cross section three on June 16, 1984 was approximately equal to that for cross section five on that date, i.e., 60-70 mm. The coarseness of the bed at cross section five on June 16, 1984 in comparison to the later dates, is probably due to the fact that the discharge then was much higher, due to snowmelt, than later on (see Fig. 8).

The bed material size distributions in cross section seven did not vary much from July, 1984 to August, 1984. It was not affected by the change in location of Roaring River flows as much as the upper cross sections (three and five). Both before and after July 24, 1984 cross section seven experienced sediment input from the Roaring River. Thus,





the slight coarsening seen on August 21, 1984 is perhaps due to the fact that a thunderstorm, causing sheet erosion on the fan, occurred closer in time to July 19, 1984 than a thunderstorm to August 21, 1984. With more time between thunderstorm and sample collection in August, the Fall River had a greater chance to flush out the sediment carried into the cross section, and thereby coarsen its bed.

Cross section nine was located downstream of almost all of the Roaring River flow for the entire summer. Therefore it, like cross section seven, was not affected by the change in location of Roaring River flows. This is evidenced by the near identical bed material size distributions of July 19 and August 21, 1984. These latter dates show a finer distribution than that shown in June. This can be explained by the fact that the month of June experienced a greater average flow due to snowmelt runoff, but did not experience the thunderstorms that July and August, 1984 did. It was found that with the thunderstorms came an increase in sediment input to the test reach, caused by sheet erosion of material on the fan. Consequently, the flows just prior to June 16, 1984, with a smaller sediment load, caused the armoring of the bed which was observed on that date. July 19 and August 21, 1984 exhibit a finer bed due to the input of sediment flowing rainfall events.

Cross section eleven behaved essentially in the same way as cross section nine.

#### 4.0 APPLICATION OF THE MODELS

##### 4.1 Results of the Application

As mentioned previously, Gessler (1970) developed a prediction of the armor layer that is based on the normal probability distribution of shear stresses and on the initial grain size distribution of the



material. On May 24, 1983 the initial grain size distributions for the cross sections in the study reach were collected. Since the Lawn Lake dam break occurred in July of the previous summer, the peak snowmelt runoff for 1982 had already occurred and so the May 24, 1983 date was prior to the 1983 runoff, which caused the armoring of the Fall River bed at the toe of the alluvial fan. Table 3 displays the initial grain size distributions for the five cross sections and Fig. 9 shows them graphically.

Table 3. Initial Grain Size Distribution

	Cross Sect. 3	Cross Sect. 5	Cross Sect. 7	Cross Sect. 9	Cross Sect. 11
d, mm	% Finer	% Finer	% Finer	% Finer	% Finer
2	0	1	5	3	4
2.8	3	3	13	6	9
4	4	18	20	11	10
5.6	18	34	33	17	11
8	22	45	43	20	20
11.2	41	53	49	38	21
16	63	61	52	53	21
22.5	81	78	56	65	48
32	92	90	71	80	59
45	98	96	85	95	82
64	99	99	100	98	96
90	100	100	100	100	100

Appendix A lists the detailed procedure followed in predicting the size distribution of the armor layer using both Gessler's model and Shen's modification to Gessler's work. The predicted mean diameter, or  $d_{50}$ , of the armor layer for each cross section using both models are compared with the actual values measured at the site, in Table 4. Observed mean diameters were chosen from the dates that showed the coarsest distribution. The larger the  $d_{50}$ , the closer it is to the



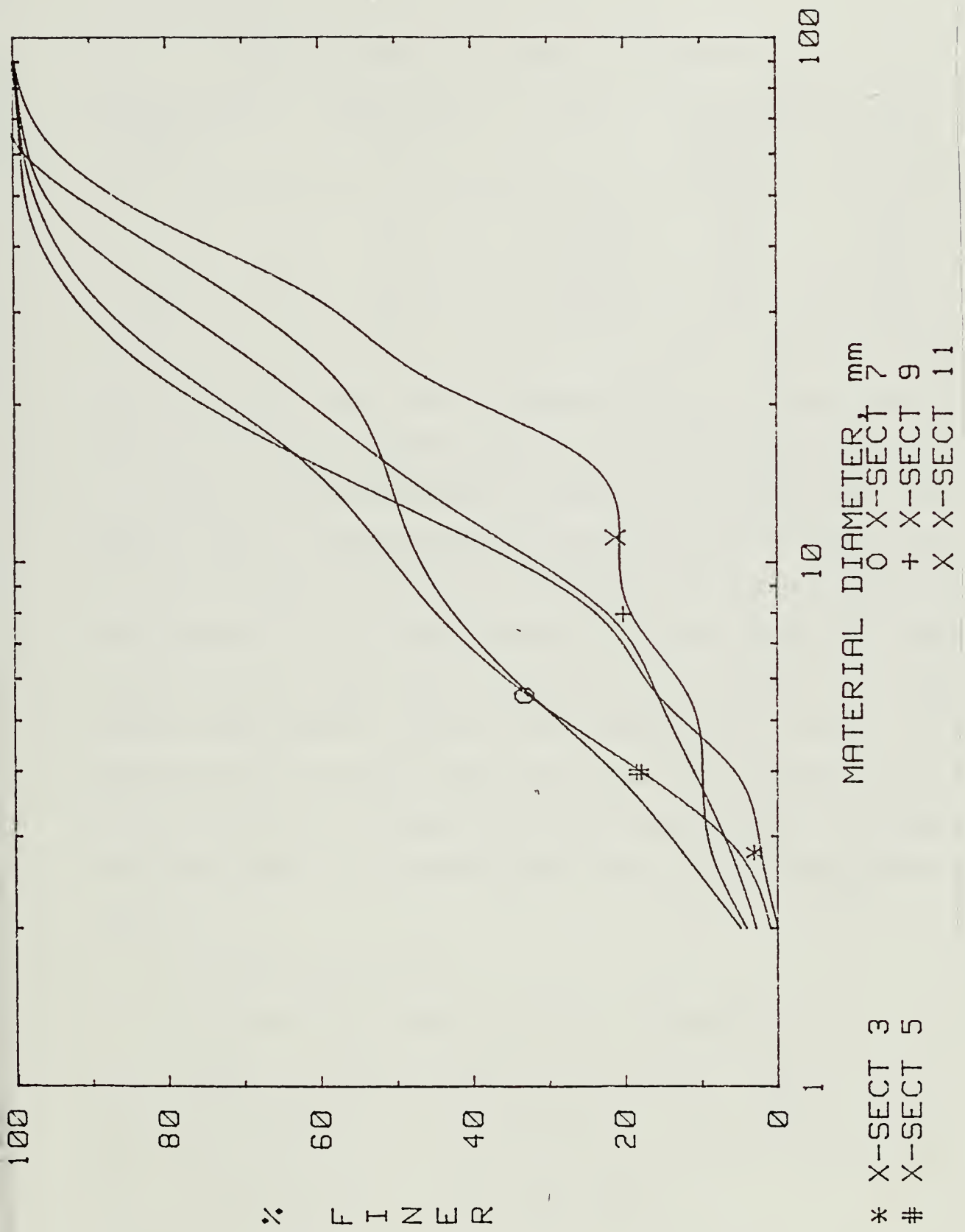


Figure 9. Initial Grain Size Distribution



Table 4. Comparison of Observed and Predicted  $d_{50}$ 

Cross Section Number	Observed $d_{50}$ mm	Date	Predicted $d_{50}$ , mm	
			(Gessler)	(Shen)
3	47	7/19/84	20	25
5	66	6/16/84	24	30
7	42	8/21/84	41	41
9	46	6/16/84	31	31
11	59	6/16/84	41	41

$d_{50}$  of the final armor coat. The smaller the  $d_{50}$ , the more affected the cross section is by sediment input and temporary storage on the bed.

Clearly, the predicted values are generally much smaller than those observed. This is especially true for the upstream cross sections 3 and 5; and for cross sections 9 and 11. Predicted and observed values for cross section 7 are in close agreement. It can be seen also that results obtained using Shen's procedure do not differ from those obtained using Gessler's method at the downstream cross sections. At the upstream cross sections, whose initial grain size distributions were finer than those of the downstream cross sections, the results obtained from Shen's model are 25 percent higher, and are closer to the measured results.

#### 4.2 Discussion of Results

Shen proposed that Gessler's procedure be modified in three ways. First, adjust the Shields diagram at low Reynolds numbers; second, include the hiding factor in the equation for  $q$ , the probability that a grain will stay in the bed; third, vary the coefficient of variation,  $(cv)_T$ , with the initial grain size distribution.





The first two of these modifications had no impact in this study and field situation. Any modification of the Shields diagram would occur at particle Reynolds numbers less than 200. In the test reach, the particle Reynolds numbers were all greater than 2200. In order to have particle Reynolds number less than 200, a river bed must be made of sand and be exposed to slow flows. This seldom occurs in gravel-bed streams. In addition, the use of the hiding factor in the procedure had no impact on the results. For the entire range of bed material diameters the hiding factor,  $\xi$ , was equal to 1.0.

The third modification, varying the coefficient of variation (see Table 2 in Shen, 1983), was found to have an effect in predicting the armor layer of the study reach. This was true for the upstream cross sections, where initial grain size distributions were finer than those for the downstream cross sections. The initial grain size distributions were, however, just fine enough to have an effect. If they would have been five millimeters coarser, no impact from the nonconstant coefficient of variation would have been realized (see Appendix A).

The application of both procedures yielded predictions of the armor layer which were much finer than those observed. Both are functions of the probability of staying for a particle and of the initial grain size distribution. The probability of staying is based on some hydraulic characteristics, such as hydraulic radius, slope of the bed and velocity of flow, and the size of the bed material. The hydraulic radii are presented in Appendix A, Table 5; the bed slope is calculated from Biedenharn (1983); and the velocity is calculated in Appendix A for the different hydraulic radii. Since these parameters can be characterized accurately enough in comparison to the model's sensitivity to them, most



of the discrepancy between predicted and observed values comes from the accuracy of the initial grain size distribution. This was measured from the Fall River bed at the toe of the alluvial fan. The composition of the fan at this location is finer than it is further upstream, as would be perceived logically. The Lawn Lake floodwaters dumped the larger particles as soon as it slowed down after leaving the constricted Roaring River valley. The smaller particles, which made the initial grain size distribution, were carried further, to the confluence of the Roaring and Fall Rivers.

The largest particles in the initial grain size distribution were less than 90 mm in diameter. On the other hand, cobbles were found in the bed of the study reach in 1984 which were larger than 128 mm. This suggests that the bed of the Fall River in this reach is the same bed that existed prior to the flood and that degradation has progressed to the level of the old channel bed. Consequently, the bed material is not a part of the alluvial fan. This bed is composed of glaciated material and is heavily armored. No further degradation beyond the armor layer will occur. The Lawn Lake flood was, after all, much larger than any historical event and it did not break up the bed in this reach. Any movement, therefore, of the Fall River in this location will occur laterally, and not vertically.

## 5.0 SUMMARY

The very dynamic nature of the alluvial fan in carrying sediment into the portion of the Fall River located at its toe provided a good opportunity to study the armoring process.

A discussion on the differences between "armored" and "paved" as used to describe gravel beds was presented. The authors chose to use



"armored" to describe a bed that was permanent, that would not be broken by even very large historic events. In addition, the process of armor-ing was described and Gessler's (1970) approach to predicting the armor layer was presented. Shen's (1983) modification to Gessler's work was described.

Data were collected during the summer of 1984 to describe the composition of the bed in the study reach. It was found that the bed material was affected primarily by thunderstorm events that brought material into the reach from the alluvial fan. The effect on the bed in the reach of one large thunderstorm which changed the flows of the Roaring River braids across the fan was described.

Both Gessler's and Shen's approaches to predicting the armor layer were applied. The results were compared to the data which were collected. It was found that the two approaches yielded essentially the same results, which underestimated the  $D_{50}$  for the armor layer.

Biedenharn (1983) stated that, "because of the highly variable nature of the Roaring River as it wanders across the alluvial fan, it is possible that the armoring trends noted this summer may be completely different in years to come." This proved to be quite true. Moreover, further study of the armoring in this location is warranted by the dynamics of the system.



## BIBLIOGRAPHY

- ASCE Task Committee for the Preparation of the Manual on Sedimentation of the Sedimentation Committee of the Hydraulics Division, Vanoni, V. A., Editor, 1975, "Sedimentation Engineering," ASCE.
- Biedenharn, D. S., 1983, "Bed Material Analysis on the Fall River," Water Resources Field Support Laboratory, National Park Service, WRFSL Project Report No. 83-6P.
- Bray, D. I., and Church, M., 1980, "Armored Versus Paved Gravel Beds," Journal of the Hydraulics Division, ASCE, Vol. 106, No. HY11, pp. 1937-1940.
- Gessler, J., 1970, "Self-Stabilizing Tendencies of Alluvial Channels," Journal of the Waterways and Harbors Division, ASCE, Vol. 96, No. WW2, pp. 235-249.
- Hey, R. D., and Thorne, C. R., 1983, "Accuracy of Surface Samples From Gravel Bed Material," Journal of the Hydraulics Division, ASCE, Vol. 109, No. 6, pp. 842-851.
- Kellerhals, R., and Bray, D. I., 1971, "Sampling Procedures for Coarse Fluvial Sediments," Journal of the Hydraulics Division, ASCE, Vol. 97, No. HY8, pp. 1165-1179.
- Parker, G., 1981, Discussion of "Armored Versus Paved Gravel Beds," Bray and Church (1980), Journal of the Hydraulics Division, ASCE, Vol. 107, No. HY9, pp. 1120-1121.
- Pitlick, J., 1985, "The Effect of a Major Sediment Influx on Fall River, Colorado," M.S. Thesis, Colorado State University, pp. 5, 14, 34, 115, 116.
- Shen, H. W., and Lu, J., 1983, "Development and Prediction of Bed Armoring," Journal of the Hydraulics Division, ASCE, Vol. 109, No. 4, pp. 611-629.





## APPENDIX A

Procedure for Calculating the Size Distribution of the Armor Layer



Given: Initial Grain Size Distribution,  $P_o$ ; Hydraulic Radius,  $R$ ; Bed Slope,  $S$ ; Velocity of Flow,  $v$ .

Gessler's Method:

1. Calculate  $\bar{\tau} = \gamma RS$ .
2. Calculate  $R = v d_s / v$ ;  $v = \frac{1.49}{n} R^{2/3} S^{1/2}$ ,  $v$  = kinematic viscosity of water.
3. From Shields Diagram, using  $R$ , find  $\tau_{*c}$  and calculate  $\tau_c = d_s (\gamma_s - \gamma) (\tau_{*c})$ .
4. Calculate  $\tau_c / \bar{\tau}$ .
5. Find  $q$  using normal probability tables (the area under the normal probability curve); for upper limit,  $z$ , use

$$\frac{\tau_c / \bar{\tau} - 1}{cv}, \quad cv = \frac{\sigma}{\bar{\tau}} = 0.57.$$

6. Set up table as shown in Example 1 below and calculate

$$q \Delta P_o, \Delta P_{a_i} = \frac{q \Delta P_{o_i}}{\sum q \Delta P_o} \quad \text{and} \quad P_a.$$

Shen's Method:

1. Calculate  $\bar{\tau}$ .
2. Calculate  $R$ .
3. Using modified Shields Diagram (Shen, 1983) find  $\tau_c$ .
4. Compute  $\xi$  as outlined in ASCE Task Committee, Sedimentation Engineering (1975), pp. 194-200.
5. Find  $(cv)_\tau$ , (Shen, 1983).
6. Calculate  $X_u = \frac{\xi(\tau_c / \bar{\tau} - 1)}{(cv)_\tau}$ .
7. Find  $q$  using for upper limit,  $z$ ,  $X_u$ .



8. Set up table as shown in Example 2 below and calculate  $q\Delta P_o$ ,  $\Delta P_a$ , and  $P_a$ .

Table 5. Hydraulic Radii and Mean Bed Stresses for the Five Cross Sections

Cross Section	R, ft	$\bar{\tau}$ , lbs/ft <sup>2</sup>
3	1.5	0.84
5	1.25	0.70
7	1.25	0.70
9	1.25	0.70
11	1.5	0.84

Example 1. Cross Section 7 (Gessler)

$S$  (from Biedenharn, 1983) = 0.009

$$V = \frac{1.486}{n} R^{2/3} S^{1/2}, \quad n = 0.035 \text{ for gravel, cobble and boulder streams}$$

$$= 5.3 \text{ fps for } R = 1.5 \text{ ft}$$

$$= 4.7 \text{ fps for } R = 1.25 \text{ ft}$$

$$R = \frac{v d_s}{v} = 3.33(10^5) d_s \quad (d_s \text{ in ft}), \text{ for } v = 4.7 \text{ fps}$$

For  $d_s = 2 \text{ mm} = 0.00656 \text{ ft}$ ,  $R = 2187$

$$\tau_c = (\gamma_s - \gamma) d_s (\tau_{*c})_c$$

From Shields diagram,  $(\tau_{*c})_c = 0.047$ ;  $\tau_c = 4.839 d_s$

The results for this example are presented in Table 6 for several values of  $d$  and are then plotted in Figure 10 along with results for all cross sections.



Table 6. Armor Layer Computations,  $P_a$ , Cross Section 7 (Gessler)

$d$ , mm	$P_o$	$d$ , ft	$d_m$ , ft	$\tau_c$ , psf	$\tau_c/\bar{\tau}$	$q$	$q\Delta P_o$	$\Delta P_a$	$P_a$
2	0.05	0.00656	0.00788	0.038	0.05	0.05	0.004	0.017	0.00
2.8	0.013	0.00919	0.0111	0.054	0.08	0.05	0.004	0.017	0.017
4	0.20	0.0131	0.0158	0.076	0.11	0.06	0.008	0.034	0.034
5.6	0.33	0.0184	0.0223	0.108	0.15	0.07	0.007	0.030	0.068
8	0.43	0.0262	0.0315	0.152	0.22	0.09	0.005	0.021	0.098
11.2	0.49	0.0367	0.0446	0.216	0.31	0.11	0.003	0.013	0.119
16	0.52	0.0525	0.0633	0.306	0.44	0.17	0.007	0.030	0.132
22.5	0.56	0.074	0.0895	0.433	0.62	0.25	0.038	0.161	0.162
32	0.71	0.105	0.127	0.615	0.89	0.42	0.059	0.250	0.323
45	0.85	0.148	0.179	0.866	1.24	0.67	0.101	0.428	0.573
64	1.00	0.210	0.253	1.22	1.74	0.90			1.00
90		0.295							

$$\Sigma q\Delta P_o = 0.236$$

#### Example 2. Cross Section 5 (Shen)

For all  $d_s$ ,  $\xi = 1.0$  (ASCE, 1975, pp. 194-200).

From Shen (1983), Table 2,  $(cv)_\tau = 0.45$ .

$$(\tau_*)_c = 0.047, \bar{\tau} = 0.70 \text{ psf.}$$

The results for various bed material sizes,  $d$ , are given in Table 7 and plotted in Figure 11 along with the results for cross section three.





Table 7. Armor Layer Computations,  $P_a$ , Cross Section 5 (Shen)

$d, \text{ft}$	$P_o$	$d_m, \text{ft}$	$\tau_c / \bar{\tau}$	$X_u$	$q$	$q\Delta P_o$	$\Delta P_a$	$P_a$
0.00656	0.01	0.00788	0.05	-2.11	0.017	0.0003	0.003	0.00
0.00919	0.03	0.0111	0.08	-2.04	0.021	0.003	0.026	0.003
0.0131	0.18	0.0158	0.11	-1.98	0.024	0.004	0.035	0.029
0.0184	0.34	0.0223	0.15	-1.89	0.029	0.003	0.026	0.064
0.0262	0.45	0.0315	0.22	-1.73	0.042	0.003	0.026	0.090
0.0367	0.53	0.0446	0.31	-1.53	0.063	0.005	0.043	0.116
0.0525	0.61	0.0633	0.44	-1.24	0.108	0.018	0.157	0.159
0.074	0.78	0.0895	0.62	-0.84	0.201	0.024	0.209	0.316
0.105	0.90	0.127	0.89	-0.24	0.405	0.024	0.209	0.525
0.148	0.96	0.179	1.24	0.53	0.702	0.021	0.183	0.734
0.210	0.99	0.253	1.74	1.64	0.950	0.010	0.087	0.917
0.295	1.00							1.000

$$\Sigma q\Delta P_o = 0.115$$



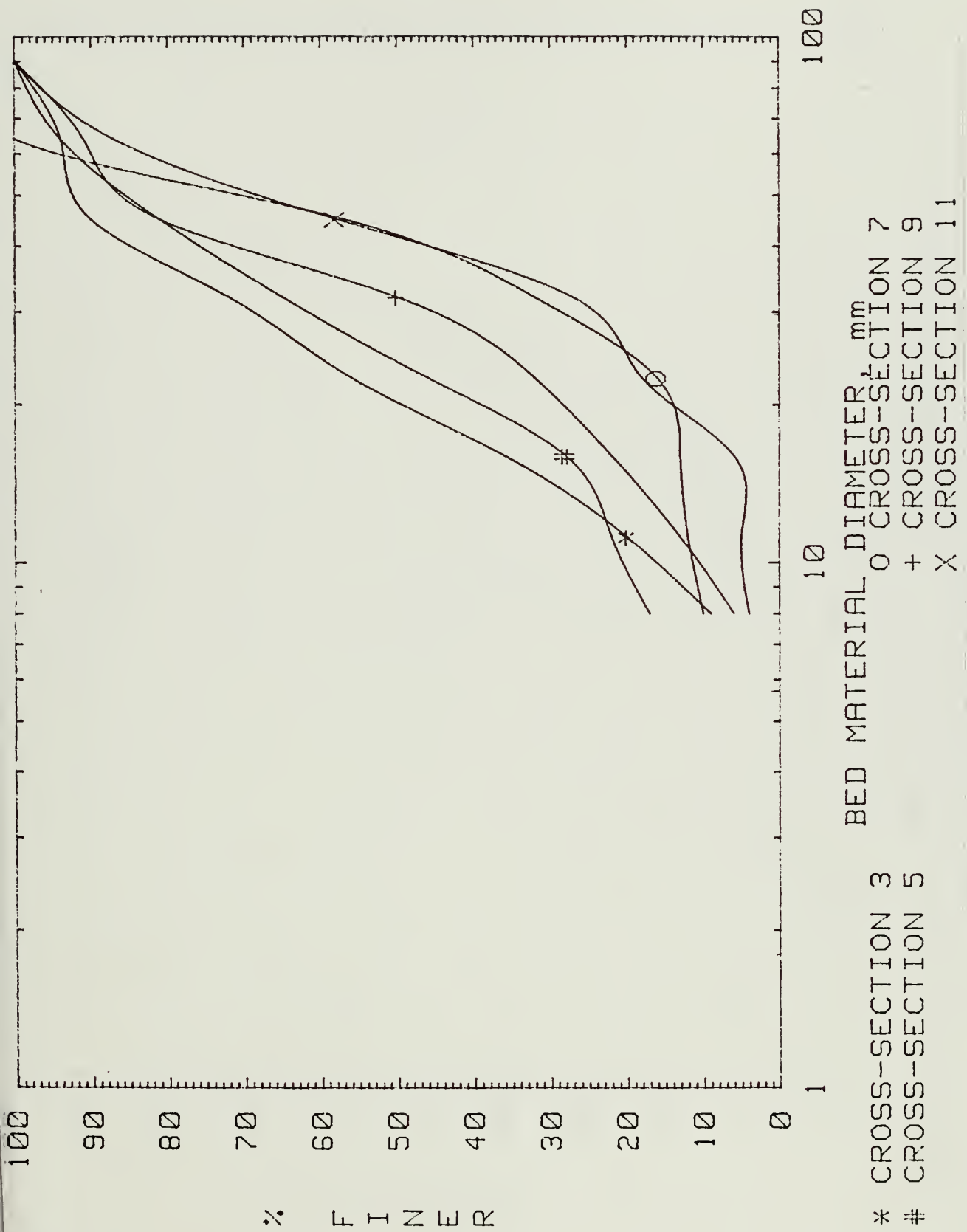


Figure 10. Prediction of Armor Layer (Gessler)



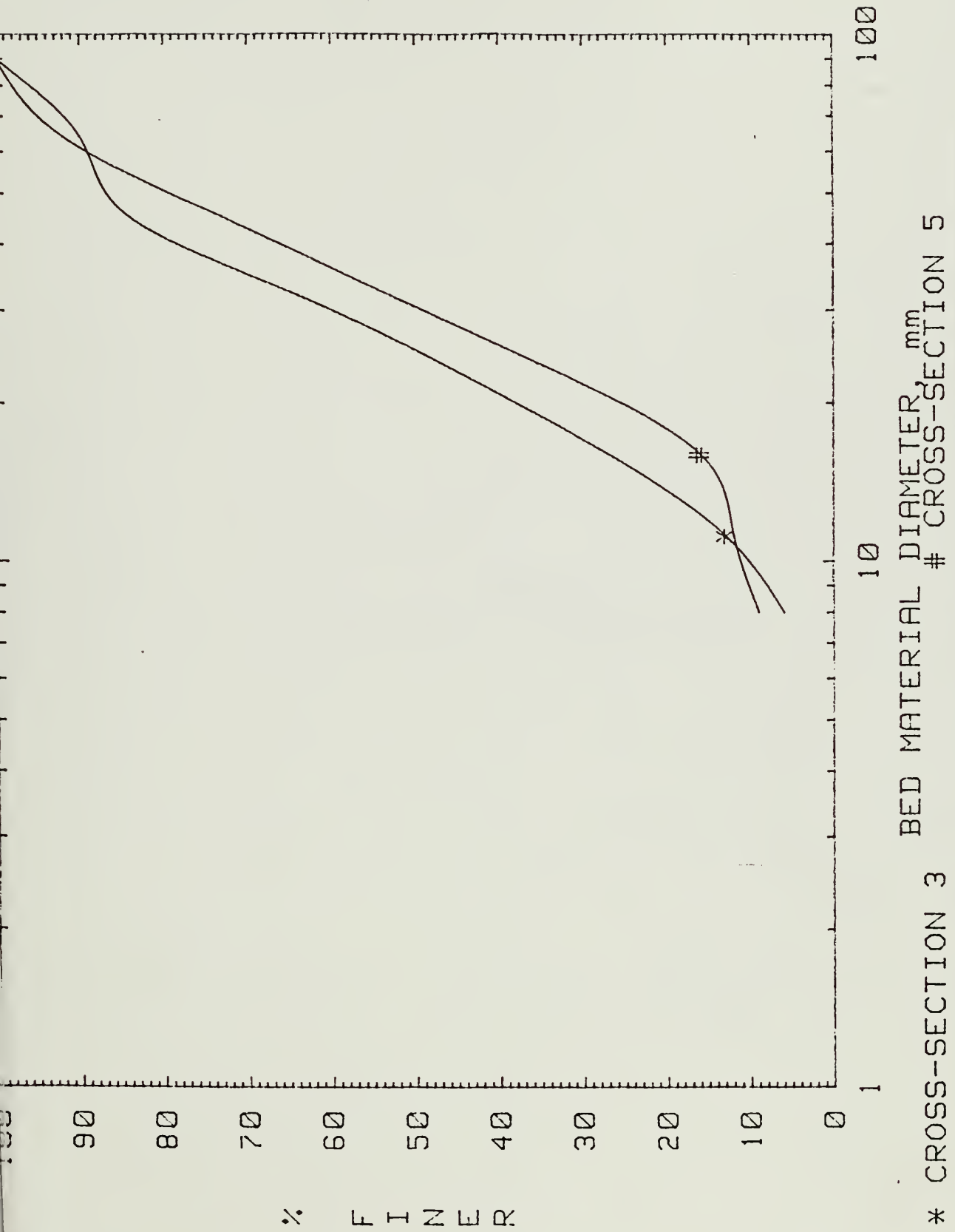


Figure 11. Prediction of Armor Layer (Shen)



APPENDIX B

1983 Results from Biedenharn (1983)





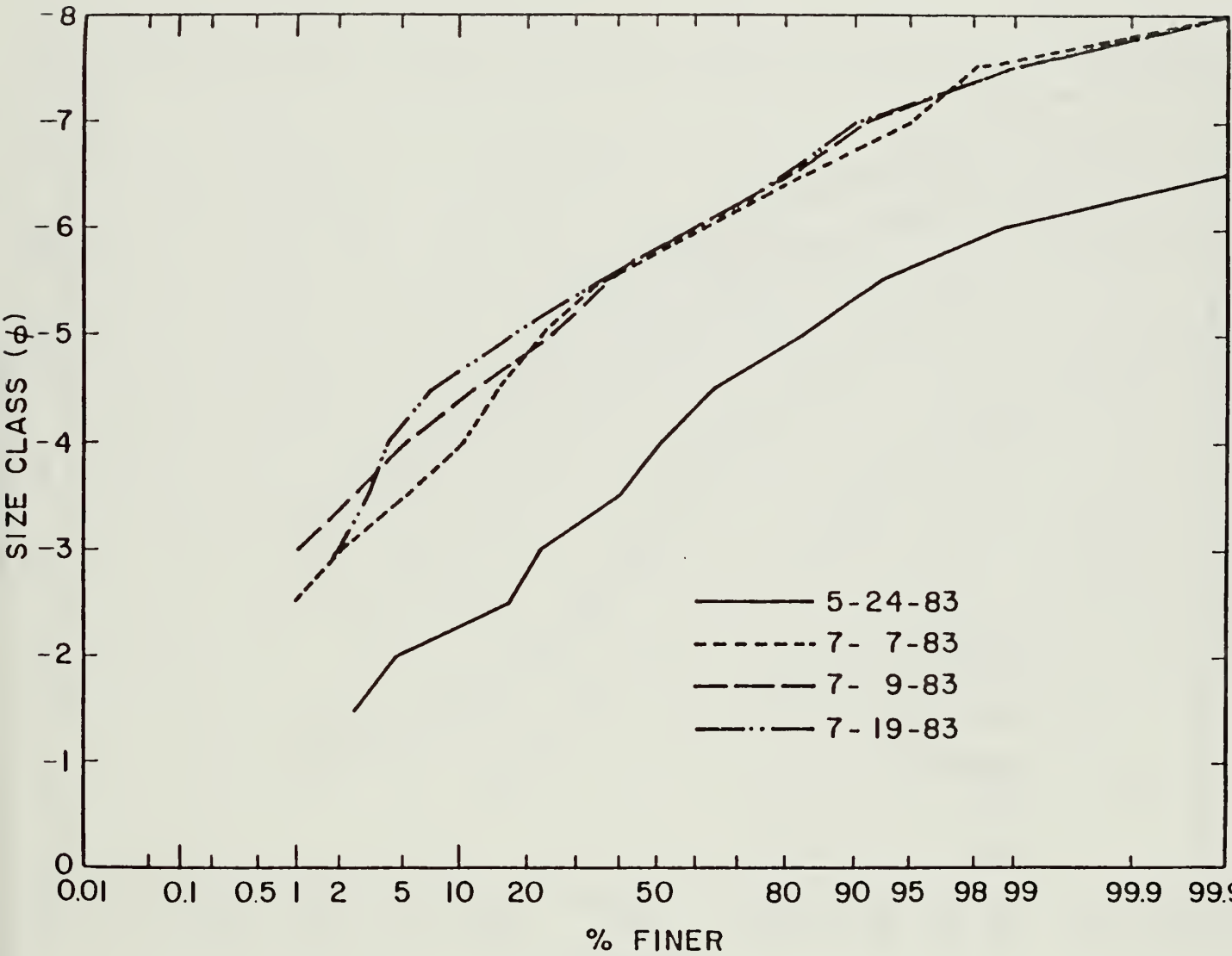


Figure 12. Size Distribution Curve, Cross Section 2, Biedenharn (1983)



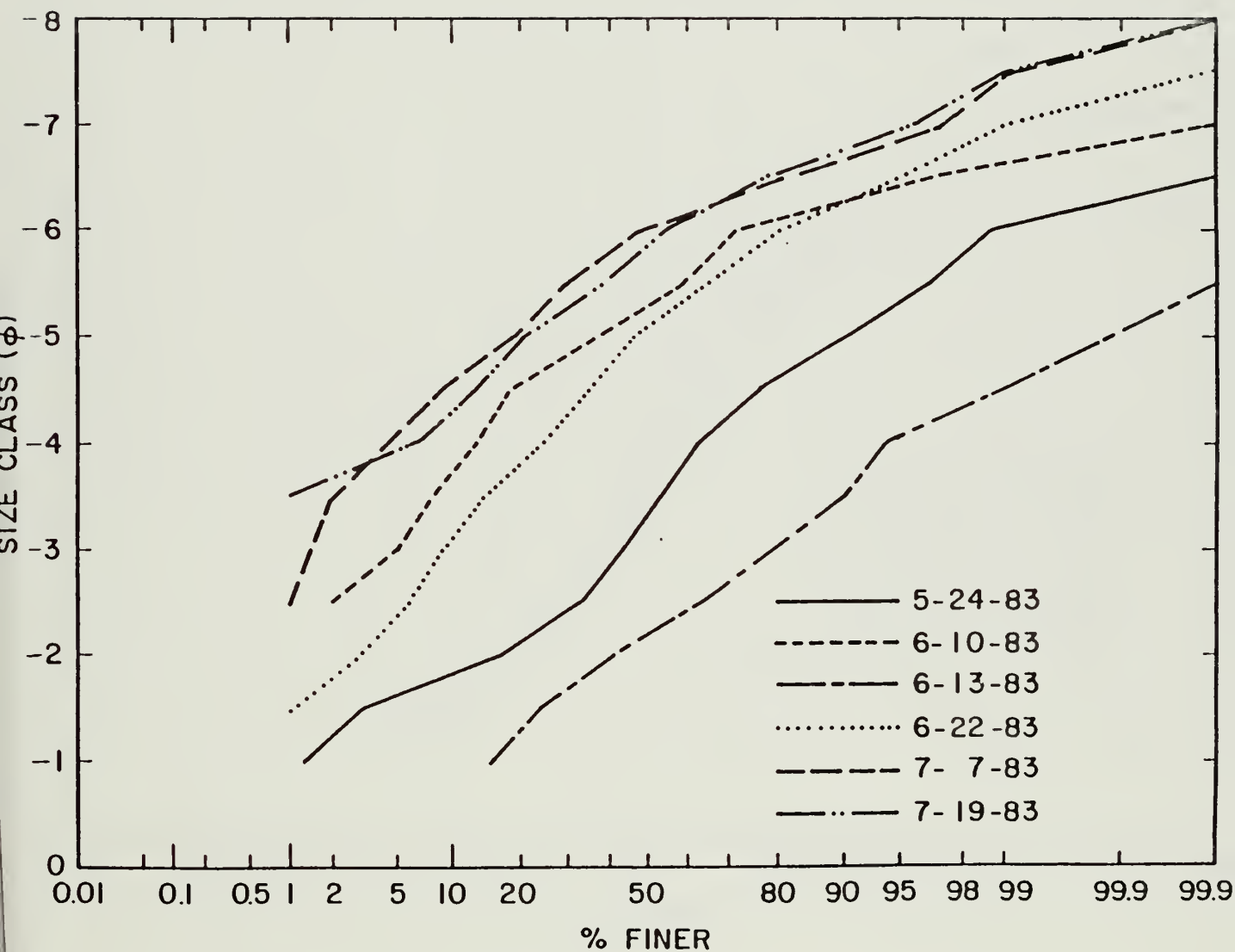


Figure 13. Size Distribution Curve, Cross Section 4, Biedenharn (1983)



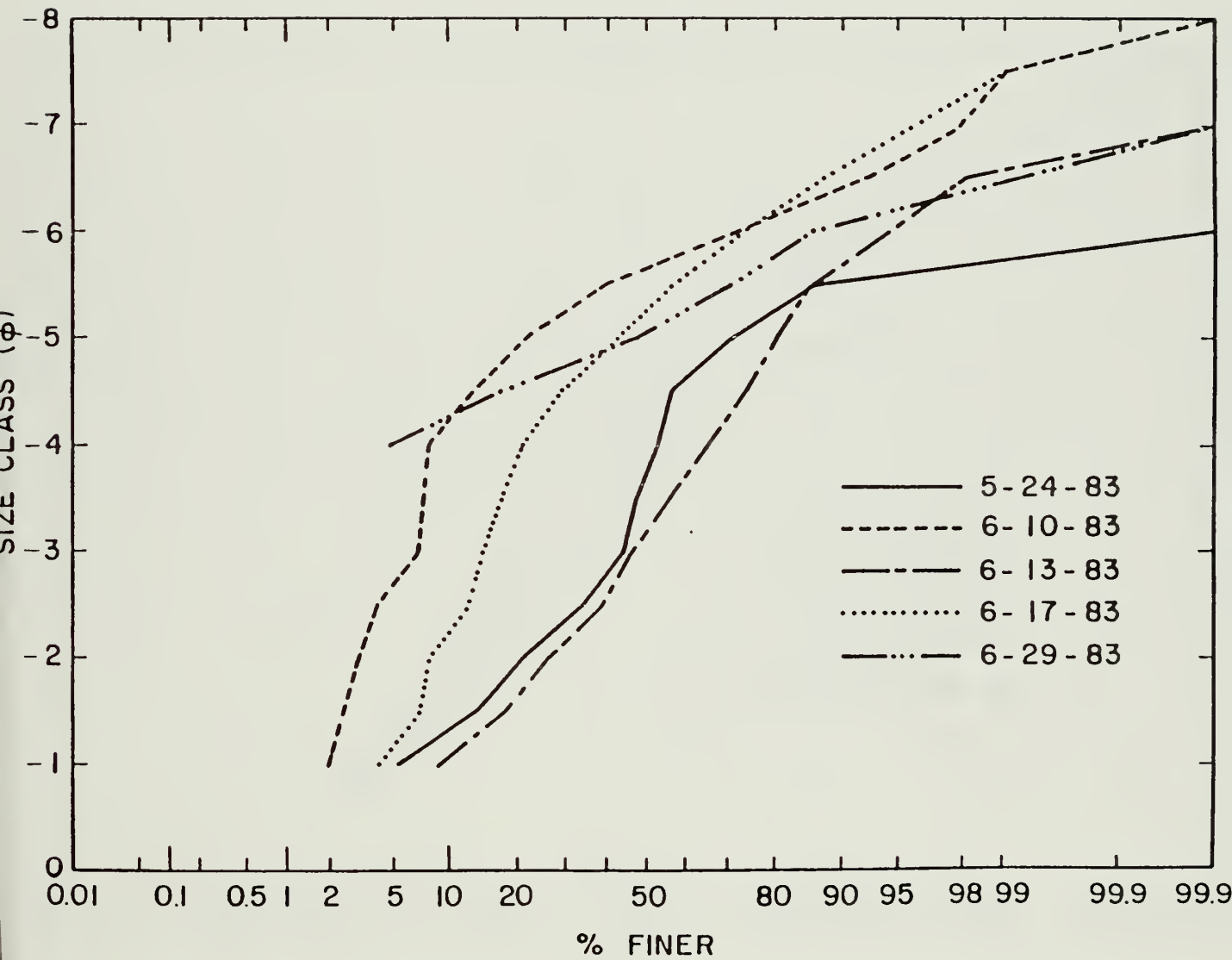


Figure 14. Size Distribution Curve, Cross Section 6, Biedenharn (1983)



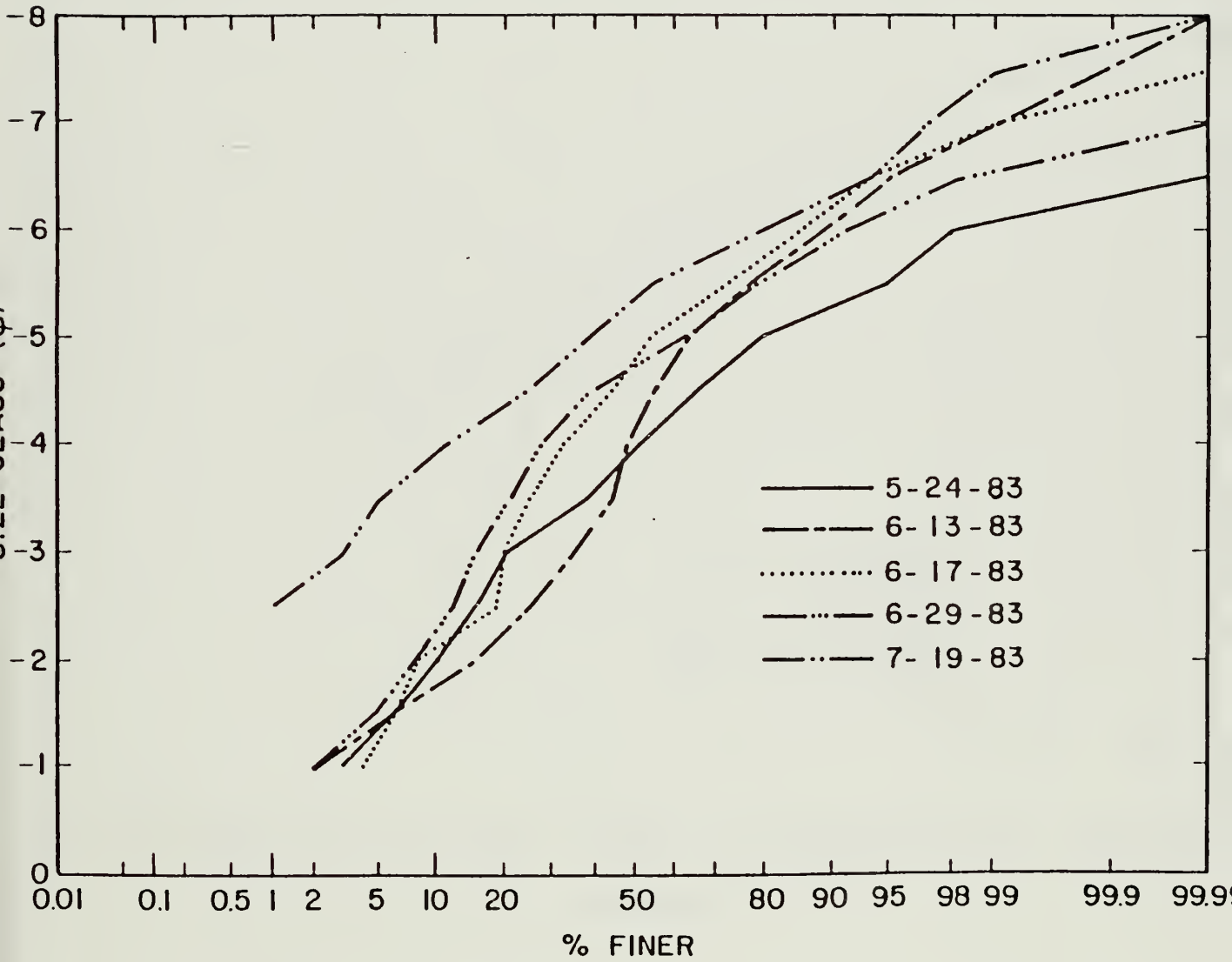


Figure 15. Size Distribution Curve, Cross Section 9, Biedenharn (1983)





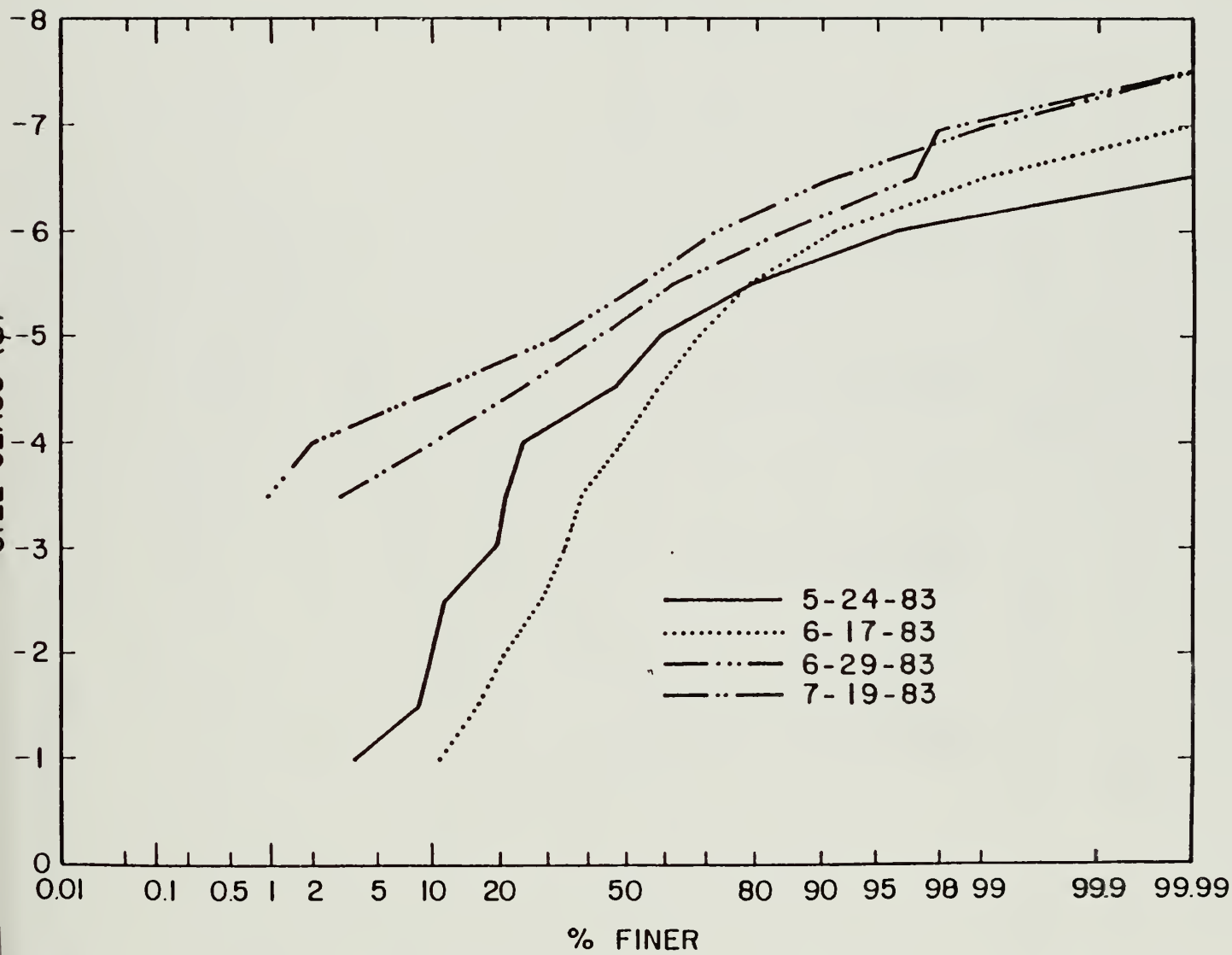


Figure 16. Size Distribution Curve, Cross Section 11, Biedenharn (1983)



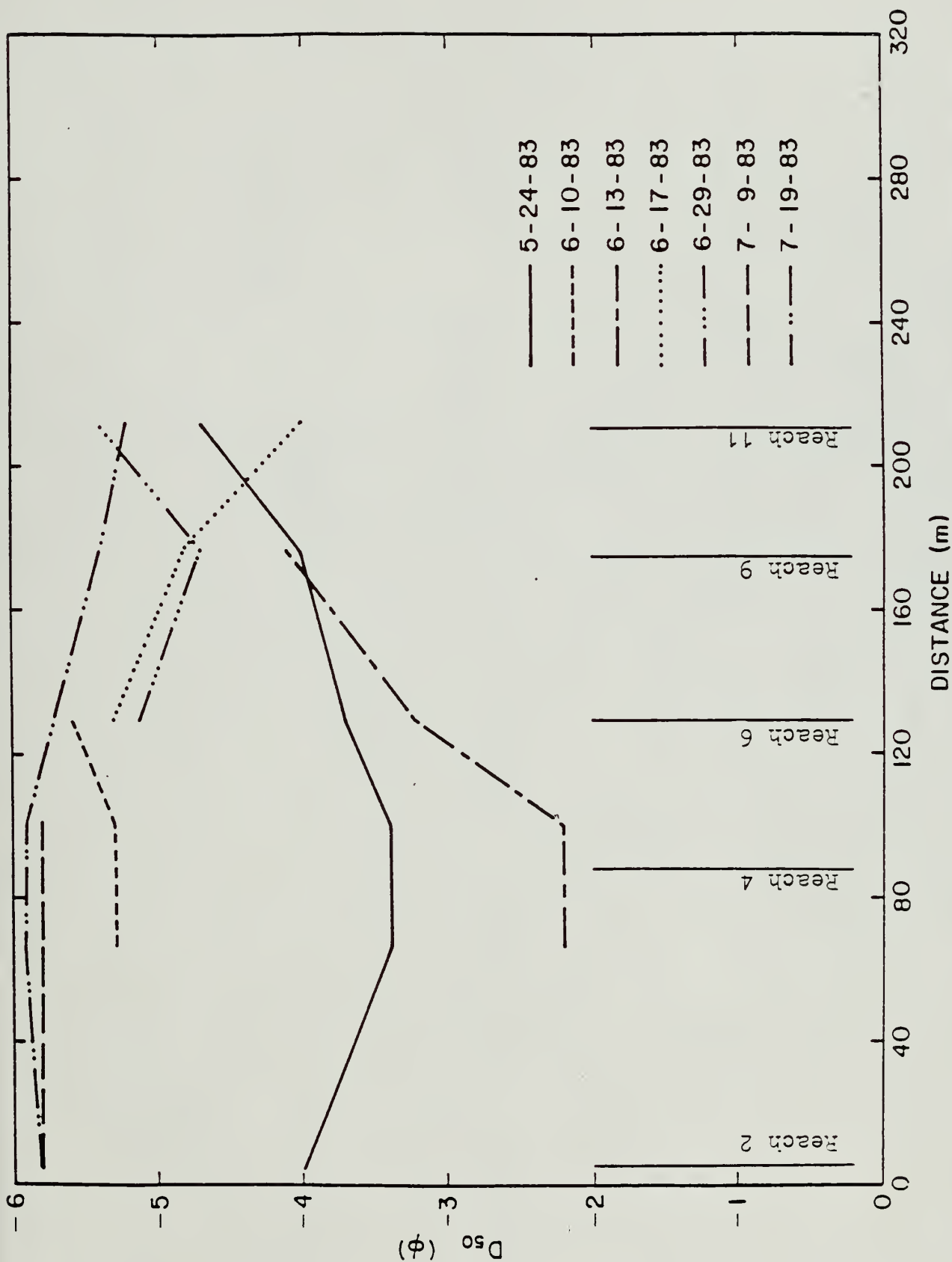


Figure 17. Variation in  $d_{50}$ , Biedenharn (1983)





